

Efficient Position Determination of Highly Directional RF Emitters via Iterated Beampattern Analysis

Fraser Williams, Student Member, IEEE
Queensland University of Technology, Brisbane, Australia

Akila Pemasiri
Queensland University of Technology, Brisbane, Australia

Dharmika Jayalath, Senior Member, IEEE
Queensland University of Technology, Brisbane, Australia

Terrence Martin
Revolution Aerospace, Brisbane, Australia

Clinton Fookes, Senior Member, IEEE
Queensland University of Technology, Brisbane, Australia

Abstract— The localization of RF emitters has attracted significant attention particularly within the domain of electronic warfare. Most localization methods found in open literature are based on omnidirectional emitters. Directional emitters significantly modulate received signal strength (RSS) resulting in degraded performance for localization techniques not modeling this behavior. This paper introduces a direct position determination (DPD) approach utilizing RSS information and adaptive beamforming to localize emitters at very low signal-to-noise-ratio (SNR). The technique is then applied to directional emitters taking the imposed RSS modulation into account using a beampattern library. This results in significantly improved localization region confidence as compared to omnidirectional assumption approaches.

Index Terms— Array processing, direct position determination, emitter localization, received signal strength, directional emitter

I. Introduction

Passive localization of radio emitters is an important step in applications such as navigation, telecommunications, and electronic warfare. This can be accomplished through the use of multiple spatially distributed receivers correlating measurements to a model of signal transformations [1], [2]. Examples of these measurements include time difference of arrival (TDOA) [1], beamforming through angle of arrival (AOA) [2], [3], Doppler shift with frequency difference of arrival (FDOA) [4]–[6], and received signal strength (RSS) [7], [8]. The use of RSS information is of particular interest for low cost, simple

receiver implementations due to its minimal hardware requirements [9], which enable them to be utilized on low size weight and power (SWaP) devices.

Signal transformations that modify the received signal strength include channel effects such as path loss, shadowing, and multipath reflections [10]. Many common radio-based tasks are enabled or greatly enhanced by the preferential, directional emission of electromagnetic energy such as long distance communications, spatial multiplexing, radar, and jamming [11], [12]. Transmissions are modulated by a beampattern resulting from a directive antenna or phased array. Consequently, approaches assuming omnidirectional emissions therefore contend with a significant source of RSS induced error, as demonstrated in this paper.

Applications such as the localization and suppression of GPS jammers and other undesirable emissions may ultimately require physical intervention from law enforcement personnel. As such methods decreasing the number and breadth of viable emitter regions present in the localization heatmap minimize resources expended and time-to-action for suppression. This includes minimising false regions of high confidence which may appear due to the nature of directional emitters supplying some receivers less information than is available from omnidirectional emitters.

To the best of the authors' knowledge, no existing models in the current literature of direct estimation approaches consider directionality-induced limitations.

Considering directionality-induced limitations can be approached through the lens of direct position determination (DPD), which directly employs a physics based model into a maximum-likelihood estimation (MLE) of emitter position, in contrast to traditional 2-step localization which derives intermediary parameters that are subsequently used for estimation [2]. DPD-based methods have recently been shown to improve localisation accuracy at moderately low signal-to-noise ratio (SNR) conditions by incorporating path loss into the transformation model [8], [13]. Without loss of generality, the path loss exponent is assumed to be 2, corresponding to free space propagation. However, specific path loss models can be used to obtain more accurate estimations considering practical environments when necessary [9], [14].

In this paper, we propose the RSS to be modulated by the transmitters' directional gain to account for the introduced deviation. However, the unknown emitter can have any antenna gain pattern, or be assumed to be of some common pattern, and can be oriented in any direction. Therefore the emitter beampattern also needs to be estimated, greatly broadening the potential search space for direct methods and increasing computational cost. This paper employs a library of expected beampatterns for a target class - such as commercial implementations of a system using linear array beamforming or other directional antenna - to constrain the search. This approach reduces the computational cost by iteratively estimating beampattern and directly localizing the emitter.

Contributions from this paper include:

- An enhanced emitter RSS-beampattern aware direct position determination method via iterated estimation, increasing localization accuracy and decreasing uncertainty.
- Analysis of an MVDR enhanced RSS array based localization method demonstrating improved performance for omnidirectional emissions.
- Analysis of a beampattern estimation strategy using a library of generic antenna configurations for emitters.
- Performance analysis of RSS-beampattern contributions to two common representative scenarios: a highly directional radar placed away from receivers, and a directive communication system surrounded by receivers.

Notation

Vectors and matrices are represented by bold lower-case and upper-case respectively, with (\cdot) denoting the discrete Fourier transform, $\|\cdot\|$ the l^2 norm, $(\cdot)^T$ the transpose, $(\cdot)^H$ the conjugate transpose, $\text{diag}\{\cdot\}$ the vector to diagonal matrix operator, and \otimes the Kronecker product.

II. Problem Formulation

Consider a stationary directional emitter, and L spatially distributed receivers each equipped with an antenna array having M elements. The signal received by the l -th receiver is given by,

$$\mathbf{r}_l(t) = b_l d_l(\mathbf{p}) g_l(\phi, \theta_l(\mathbf{p})) \mathbf{a}_l(\mathbf{p}) s(t - \tau_l(\mathbf{p}) - t_0) + \mathbf{n}_l(t), \quad (1)$$

where $\mathbf{r}_l(t)$ is the $M \times 1$ received signal vector at time t , b_l is the complex channel attenuation factor, $d_l(\mathbf{p})$ is the path attenuation of the signal, $\theta_l(\mathbf{p})$ is the angle between the transmit and receiver position, ϕ is the transmitter orientation, $g_l(\phi, \theta_l(\mathbf{p}))$ is the complex gain derived from the transmitter beampattern, $\mathbf{a}_l(\mathbf{p})$ is the receiver steering vector, $s(t - \tau_l(\mathbf{p}) - t_0)$ is the signal waveform at time t transmitted at t_0 , delayed by $\tau_l(\mathbf{p})$, and $\mathbf{n}_l(t)$ represents noise and interference at the l -th receiver.

The path attenuation $d_l(\mathbf{p})$ is given by,

$$d_l(\mathbf{p}) = \sqrt{\frac{P_T G_T G_R \lambda^2}{(4\pi \|\mathbf{p} - \mathbf{u}_l\|)^2 L_l}}, \quad (2)$$

where P_T is the transmit power, G_T the gain of the emitter, G_R the gain of the receiver for an individual antenna element, λ the radio wavelength, L_l system losses such as filter insertion loss, and $\|\mathbf{p} - \mathbf{u}_l\|$ the distance between emitter and receiver.

Expressing (1) in frequency domain we have,

$$\tilde{\mathbf{r}}_l(k) = b_l d_l(\mathbf{p}) g_l(\phi, \theta_l(\mathbf{p})) \mathbf{a}_l(\mathbf{p}) \tilde{s}(k) e^{-j\omega_k[\tau_l(\mathbf{p}) + t_0]} + \tilde{\mathbf{n}}_l(k) \quad (3)$$

$$\omega_k \triangleq \frac{2\pi k}{N_s T}, \quad (4)$$

where N_s is the number of signal samples, T is the sampling period, and k is the discrete frequency bin.

A least-squares maximum-likelihood approach is used to estimate \mathbf{p} . To maximize clarity, we define the following,

$$\mathbf{d}(\mathbf{p}) \triangleq [d_1(\mathbf{p}) \dots d_L(\mathbf{p})]^T \quad (5)$$

$$g_l(\phi, \theta(\mathbf{p})) \triangleq [g_1(\phi, \theta_1(\mathbf{p})) \dots g_L(\phi, \theta_L(\mathbf{p}))]^T \quad (6)$$

$$\gamma(\phi, \mathbf{p}) \triangleq \mathbf{g}(\phi, \theta(\mathbf{p})) \odot \mathbf{d}(\mathbf{p}) \quad (7)$$

$$\mathbf{a}(\mathbf{p}, k) \triangleq [e^{-j\omega_k \tau_1(\mathbf{p})} \mathbf{a}_1^T(\mathbf{p}) \dots e^{-j\omega_k \tau_L(\mathbf{p})} \mathbf{a}_L^T(\mathbf{p})]^T \quad (8)$$

$$\mathbf{A}(\mathbf{p}, k) \triangleq \text{diag}\{\mathbf{a}(\mathbf{p}, k)\} \quad (9)$$

$$\mathbf{c}(\mathbf{p}, k) \triangleq \mathbf{A}(\mathbf{p}, k) \gamma(\phi, \mathbf{p}) \quad (10)$$

$$\tilde{\mathbf{r}}(k) \triangleq [\tilde{\mathbf{r}}_1^T(k) \dots \tilde{\mathbf{r}}_L^T(k)]^T. \quad (11)$$

The maximum-likelihood estimator is then given by minimising the following,

$$Q(\mathbf{p}) = \sum_{k=0}^{N_s-1} \|\tilde{\mathbf{r}}(k) - \mathbf{c}(\mathbf{p}, k) \tilde{s}(k)\|^2. \quad (12)$$

From [13] we find this equivalent to maximising the cost function $\tilde{Q}(\mathbf{p})$ given by,

$$\tilde{Q}(\mathbf{p}) = \sum_{k=0}^{N_s-1} \frac{|\mathbf{c}^H(\mathbf{p}, k) \tilde{\mathbf{r}}(k)|^2}{\|\gamma(\phi, \theta(\mathbf{p}))\|^2}. \quad (13)$$

By expanding and re-arranging we achieve the form,

$$\tilde{Q}(\mathbf{p}) = \frac{\gamma(\phi, \mathbf{p})^H \mathbf{R} \gamma(\phi, \mathbf{p})}{\|\gamma(\phi, \mathbf{p})\|}, \quad (14)$$

with,

$$\mathbf{R} \triangleq \sum_{k=0}^{N_s-1} \mathbf{A}^H(\mathbf{p}, k) \tilde{\mathbf{r}}(k) \tilde{\mathbf{r}}^H(k) \mathbf{A}(\mathbf{p}, k). \quad (15)$$

The MLE cost function presented in (13) utilises RSS information that has been shown to degrade performance at SNRs below -12 dB in [13]. This sudden degradation of performance is resultant from spuriously high values in the cost function due to noise, and can be remedied through the use of adaptive beamforming techniques.

Applying the principles of MVDR in a similar manner to [15] to (14), results in,

$$\tilde{Q}_{\text{MVDR}}(\mathbf{p}) = \left[\frac{\gamma(\phi, \theta(\mathbf{p}))^H \mathbf{R}^{-1} \gamma(\phi, \theta(\mathbf{p}))}{\|\gamma(\phi, \theta(\mathbf{p}))\|} \right]^{-1}. \quad (16)$$

The emitter position is then given by,

$$\hat{\mathbf{p}} = \arg \max_{\mathbf{p}} \tilde{Q}(\mathbf{p}). \quad (17)$$

For known emitter beampattern and orientation this can be resolved by a 2-dimensional grid search, and is of similar computational complexity to a standard DPD-based approach such as [2] with an additional ML evaluations of a beampattern function $g_l(\phi, \theta_l(\mathbf{p}))$ and associated multiplication to form $\gamma(\phi, \mathbf{p})$. This evaluation can be implemented generally via a lookup table for an arbitrary measured beampattern.

However, in the general case where the emitter beampattern and the orientation is not known, a 4-dimensional search is required to accommodate the 2 dimensions of \mathbf{p} , as well as the complex gain beampattern g and orientation ϕ . Such a search is highly undesirable as it dramatically increases the computational cost as the size of the beampattern library and grid increases. Further, the presence of highly directive beampatterns may require a finer search of emitter orientations in order to be effective, exacerbating the effect.

One solution to this problem is estimating the beampattern and orientation of the emitter separately to its position. This can be achieved by limiting the search over beampattern and orientation by first fixing an initial position. In practice this is obtained from a non-directional source localisation scheme via optimisation of some $\tilde{Q}_{\text{base}}(\mathbf{p})$, possibly $\tilde{Q}_{\text{MVDR}}(\mathbf{p})$ while setting $\gamma = \mathbf{1}_{ML}$, or through an informed choice of candidate \mathbf{p} , for example by specifying high value search areas due to the local topography or by other known constraints. This initial estimate of beampattern and orientation can then be fixed searching over position, iterating until the Euclidean distance between successive differences falls below an acceptable tolerance ε , or reaching some maximum number of iterations. Algorithm 1 details this process.

Algorithm 1 Iterated Position Estimation

Input: $r_l, \mathbf{u}_l, \varepsilon$

Output: $\hat{\mathbf{p}}$

$\hat{\mathbf{p}} = \arg \max \tilde{Q}_{\text{base}}(\mathbf{p})$

do

$\hat{\mathbf{p}}_{\text{prev}} = \hat{\mathbf{p}}$

$g_l, \phi = \arg \max \tilde{Q}_{\text{MVDR}}(\mathbf{p}, g_l, \phi) |_{\mathbf{p}=\hat{\mathbf{p}}}$

$\hat{\mathbf{p}} = \arg \max \tilde{Q}_{\text{MVDR}}(\mathbf{p}, g_l, \phi)$

while $\|\hat{\mathbf{p}} - \hat{\mathbf{p}}_{\text{prev}}\| > \varepsilon$

return $\hat{\mathbf{p}}$

III. Simulation Results

Due to the highly directive nature of the emitters evaluated in this study, several Monte Carlo simulations varying emitter position, beampattern, and orientation are used to evaluate performance. It is not possible to fully randomise these parameters simultaneously as many untenable situations would arise, such as a highly directive

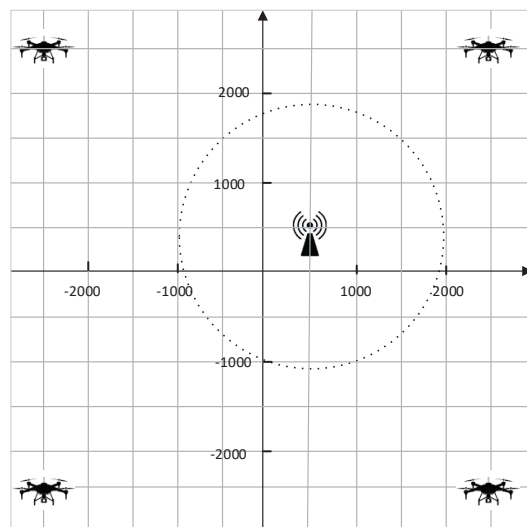


Fig. 1. Omnidirectional communication system setup.

emitter transmitting no such signal to any receivers. Non-directional DPD methods were evaluated for comparison, exploiting time delay (TDOA) and angle of arrival (AOA). Additional evaluations were conducted with received signal strength without compensation for emitter directivity (AOA-TDOA-RSS). The experiment replicates the parameters of [13], with transmitted waveform samples drawn from a circular normal distribution with bandwidth 200 kHz. $N = 32$ samples are captured from $M = 4$ linear array antenna elements having $\lambda/2$ separation. $L = 4$ receivers are distributed at fixed positions. Candidate positions are evaluated over a grid of width and height 10 km with 50 m resolution. SNR is varied between -15 dB and 0 dB in steps of 1 dB, having 250 trials each. Error is taken as the Euclidean distance between estimated and true emitter position. The final calculated error is the root mean square (RMS) of the trials for each SNR.

A. Omnidirectional Communication System

The developed cost function of (16) naturally applies in the case of omnidirectional emissions with $g_l(\phi, \theta_l(\mathbf{p})) = 1$. For many communication systems this is the primary emission mode as omnidirectional antennas are widely available, less expensive, and do not place restriction on users such as having a preferred orientation. Therefore it is imperative to evaluate the performance of localization in this scenario which may comprise the majority of detected emissions in urban environments. This experiment entails extension to that of [13] in which MVDR adaptive beamforming is used to reduce the effect of spurious noise. Receivers are placed at locations $[-2500, -2500], [-2500, 2500], [2500, -2500], [2500, 2500]m$, with transmitter placed at $[500, 500] \pm 250m$ in each coordinate. The setup is illustrated in Fig. 1.

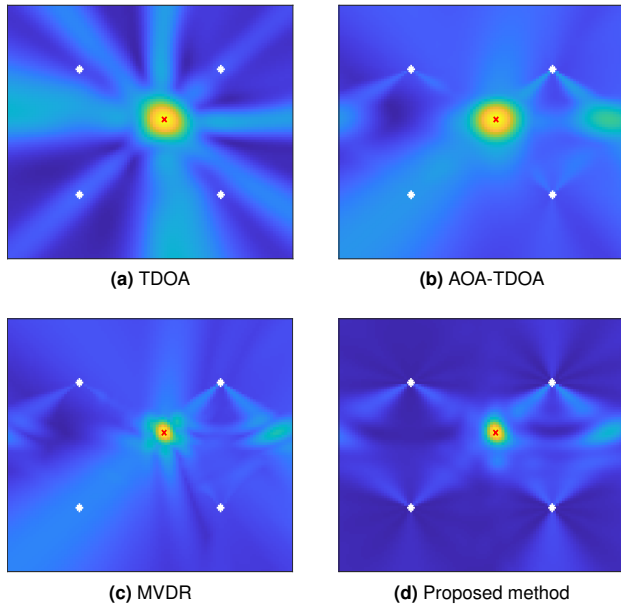


Fig. 2. Omnidirectional communication system experiment; Heatmaps of different localization methods with SNR = 30 dB, $N = 32$, $M = 4$, $L = 4$, $g_l(\phi, \theta_l(\mathbf{p})) = 1$. Grids measure 10 km x 10 km. Superimposed white symbols represent receiver positions, and the red cross represents emitter position.

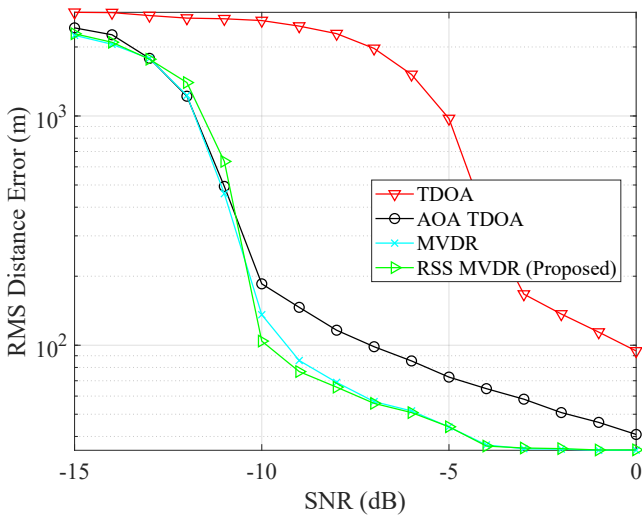


Fig. 3. Omnidirectional communication system experiment; RMS distance error vs SNR, $N = 32$, $M = 4$, $L = 4$, $M_{tx} = 16$.

Fig. (2) shows a significant qualitative improvement in the generated heatmaps when using RSS information. This improvement is evident even at low SNR where the performance of the previous RSS-inclusive techniques begin to decline significantly due to spurious noise.

The proposed cost function improves upon RMS distance error as compared to traditional, RSS array, and MVDR based approaches shown in Fig. 3. While sensitive to amplitude modulations, the enhanced resolving power has reduced uncertainty in estimation (Fig. 4).

We observe that the proposed technique exhibits improved performance even at very low SNR for certain scenarios of omnidirectional emissions. Therefore, this

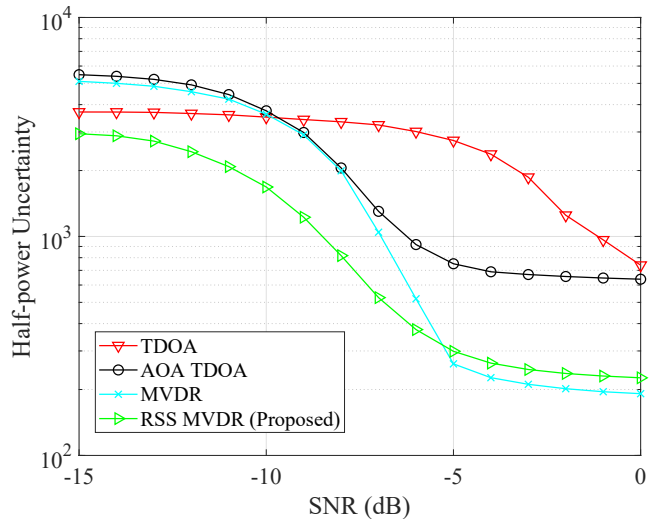


Fig. 4. Omnidirectional communication system experiment; RMS half-power uncertainty vs SNR, $N = 32$, $M = 4$, $L = 4$, $M_{tx} = 16$.

observation supports the inclusion of RSS information in the estimation model whenever possible. However, the presence of RSS modulation due to directional transmitters may significantly affect the estimation under this model. Accurate estimation of emitter beampattern is therefore critical to maintaining the enhanced performance observed in the omnidirectional case.

B. Emitter Beampattern Estimation

Successful beampattern estimation may be used to extend the MVDR RSS array enhanced technique to the case of directional emitters. The cost function (16) can be re-used in this case given an initial estimate of position. It is necessary to evaluate the cost function's effectiveness in estimating the beampattern, which also includes an estimate of emitter orientation. To do so, a small beampattern library emulating $g_l(\phi, \theta_l(\mathbf{p}))$ consisting of uniform linear arrays (ULAs) and patch antenna based ULAs (simulated as ULA without backscatter) are implemented up to 16 antenna elements. While many directional antennas exist and may be included in this library, the primary focus of this experiment lies in the width of the main lobe, the presence of nulls, and very low power (or no power) regions in the beampatterns such that receivers effectively capture uncorrelated noise.

A fixed scenario of known emitter position is constructed whilst varying emitter beampattern and orientation. Receivers are placed at $[-2500, -2500]$, $[-2500, 2500]$, $[2500, -2500]$, $[2500, 2500]$, with emitter at $[-4500, 4500]$. 250 trials are performed as SNR is varied. The predicted beampattern and orientation are selected as those maximising the cost function $\hat{Q}_{MVDR}(\mathbf{p}, g_l, \phi)$. Fig. 5 presents a sample from the beampattern library and the evaluation scenario.

Many such scenarios may result in little power delivered to some receivers. A correct estimation of emitter beampattern and orientation is expected to occur when

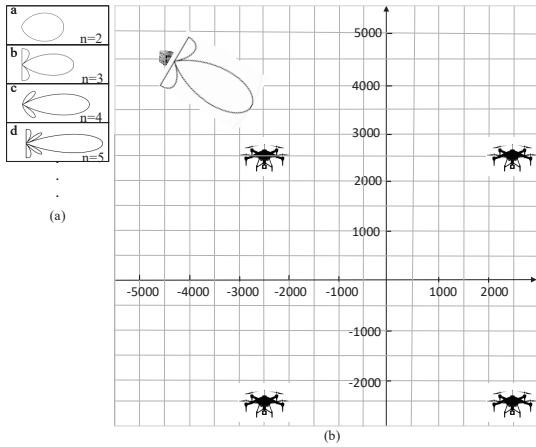


Fig. 5. Emitter beampattern estimation. UAV symbols represent receivers placed at those coordinates. (a) Sample collection of beampatterns within the library (b) Beampattern estimation setup.

given a perfect initial estimate of position, leaving only orientation and beampattern unknown in the cost function. However, it is feasible that many beampatterns may fit the captured data closely under a particular snapshot when initial position is in error, particularly as the main lobe beamwidth reduces. For example, when all receivers from a distant source exist within the main lobe of an emission it can lead to a little effective difference between the directionality imposed by a 15 element ULA or a 16 element ULA emitter. This implies that receiver diversity relative to the emitter plays a significant role in an effective estimation.

Fig. 6 shows the beampattern estimation evaluated for an index of 16 patch antenna based ULAs with an increasing number of elements. Evidently many beampatterns within the library effectively match the results even given a perfect estimation of emitter position. This can be explained as ULAs with a similar number of antenna elements form sufficiently similar beampatterns from the perspective of receivers which are contained within the main lobe. It happens that while the correct beampattern is chosen by the estimation step, nominally a 4-element ULA oriented at 330° , a number of candidates are viable with widely varying elements and orientations. The spikes in high cost correspond to the main lobe and first side lobe encompassing the majority of the receivers leading to generally lower variations in RSS due to beampattern. It is shown that no such beampatterns within our given library permit that the emitter is oriented between 70 and 230 degrees relative to the positive x-axis, corresponding to no signal arriving at the receivers. This information can be used to refine our search by cutting down the number of angles evaluated in subsequent captures, or to increase the resolution on the smaller number of viable orientations.

The quantitative performance (Fig. 7) improves with increasing SNR as expected, with the leading diagonal of true and predicted classes highlighted. Of special note

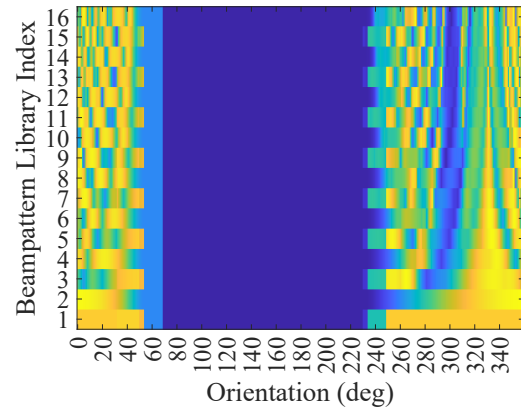


Fig. 6. Emitter beampattern estimation experiment; Heatmap of estimated class and orientation given an exact initial position of the emitter.

is the very low frequency in which the predicted class 1 (a patch antenna) is estimated regardless of SNR. All other beampatterns with higher directivity improve more significantly as SNR increases.

Similar beampatterns (as ordered next to each other in ascending number of transmit elements in a ULA) are not more often mistaken to be the true beampattern than those with a greatly varying number of elements, i.e. a 5-element ULA is most likely to be predicted to be a 5-element ULA, however a 4-element or 6-element ULA is not the second most likely candidate. This would refute the assertion that the main lobe is solely responsible to select beampattern, as similar functions whose main lobe width changes minimally to the true beampattern do not experience higher prediction frequency.

This can be explained by the constructed experiment allowing for the main lobe and first number of sidelobes of the beampattern to be spatially sampled where variation is greatest, increasing the selectivity of the process. This would demonstrate the importance of the library including realistic functions that account for side lobe behaviour.

At very high SNR, it is evident that the process converges on reliably predicting the correct beampattern from within the library. This verifies that (16) is sufficient for beampattern estimation given optimal initial position conditions in Fig. 8.

C. Highly Directive Radar System

A highly directive radar system having very thin beamwidth may result in dramatic variations in received signal strength experienced at all receivers, with some receivers existing within nulls or very low power sidelobes. This signal environment may commonly be encountered as mobile aerial receivers are progressing from their initial takeoff location into an area to be surveilled for emitters. Initially the receivers can be clumped relative to the emitter at a large distance away before later increasing their spatial diversity either naturally by approaching the location, or through purposeful distribution to enclose a location of interest.

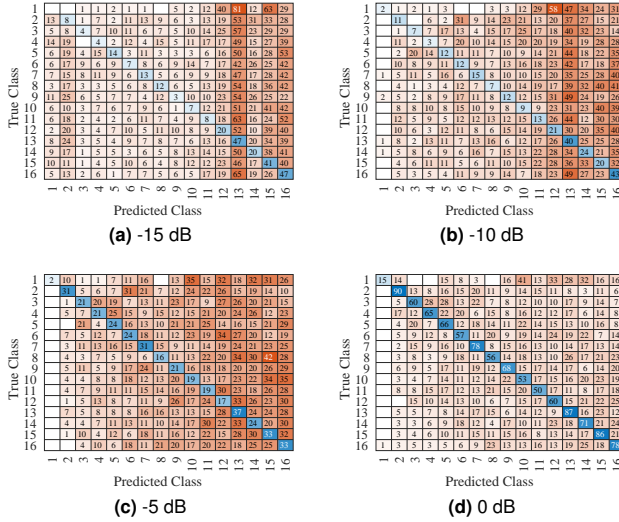


Fig. 7. Emitter beampattern estimation experiment: Confusion matrix comparing transmit beampattern and estimated beampattern at SNR levels of (a) -15 dB, (b) -10 dB, (c) -5 dB, and (d) 0 dB.

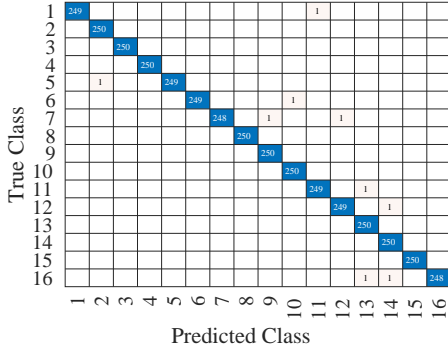


Fig. 8. Emitter beampattern estimation experiment: Confusion matrix comparing transmit beampattern and estimated beampattern at SNR of 30 dB.

Receivers are placed at locations $[-2500, -2500]$, $[-2500, 2500]$, $[2500, -2500]$, $[2500, 2500]m$, with transmitter placed at $[-4500, 4500] \pm 250m$ in each coordinate. Transmit orientation is given as $0 \pm 30^\circ$ utilising a 16-element ULA with patch antenna elements transmit pattern. The setup is illustrated in Fig. 9.

The effect of transmit beampattern on localization performance is evident even in optimal noise conditions as shown in Fig. 10. While all methods correctly estimate emitter position to within the closest evaluated cell of $50m \times 50m$ size, the viable region of estimates is dramatically reduced through consideration of the emitter beampattern. This is an important consideration for practical implementations which require high levels of confidence in the result. Further, consideration of RSS and beampattern has limited the scope of the localization estimate to a finite distance away from the receivers, in contrast to non-RSS based techniques that produce a conic viable region that increases in extent further from the receivers, providing more localized and fine grained result. To capture this observed behaviour an additional metric is considered for this analysis – half-power uncertainty

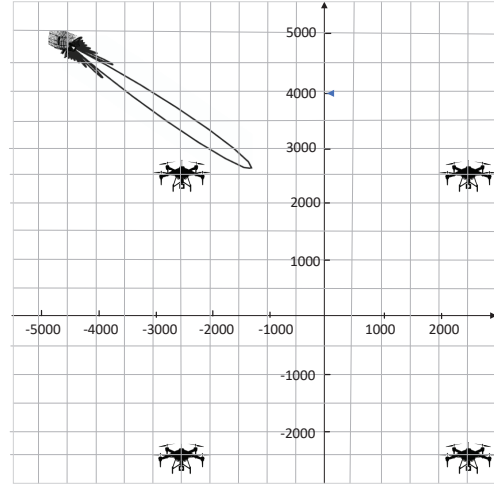


Fig. 9. Highly directive radar representative experimental setup.

– which evaluates the extent of the viable region as the number of cells that contain a cost $\hat{Q}(\mathbf{p})$ that is half-power or greater than that of the global maximum. Note that this generally corresponds to a contiguous region around the maximum, and should optimally be small, corresponding to a precise estimate.

Fig. 11 shows the localization performance of the proposed method compared to other techniques. The proposed technique's performance is on par with that of MVDR and is enhanced little by the addition of RSS information. This is explained by the lack of diversity in receiver position and relatively high performance of MVDR already. However, it is important to consider this with respect to the half-power uncertainties exhibited in Fig. 12 which show a dramatic improvement in uncertainty as SNR increases. While MVDR and the other non-RSS based techniques continue to show high uncertainty even as SNR increases, the proposed iterative technique becomes increasingly confident in its estimation as SNR increases, and the uncertainty decreases at a rate proportional to the localization RMS distance error. This substantiates that the half-power uncertainty metric fulfils its most important property of representing estimate uncertainty; if uncertainty values were to decrease disproportionate to RMS distance error, then a technique would confidently estimate incorrectly.

D. Directive Communication System

A directive communication system utilising a 4-element uniform linear array with patch antenna elements, in which all receivers intercept the signal at varying places within the main and first side lobe, is simulated. This is a realistic scenario for many long distance communications, and functions as an analog for MIMO communication and similar. This may be encountered in UAV long distance control links or directed GPS jamming.

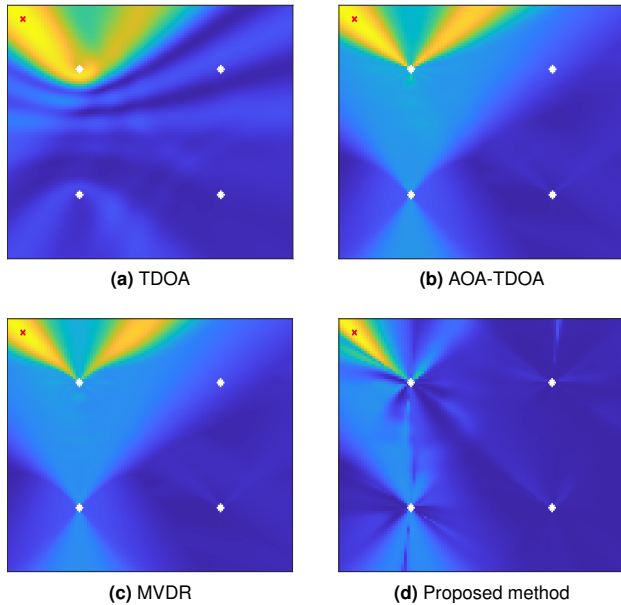


Fig. 10. Highly directive emitter experiment; Heatmaps of different localization methods with SNR = 30 dB, $N = 32$, $M = 4$, $L = 4$, $M_{tx} = 16$ ULA transmit beam pattern. Grids measure 10 km x 10 km. Superimposed white symbols represent receiver positions, and the red cross represents emitter position.

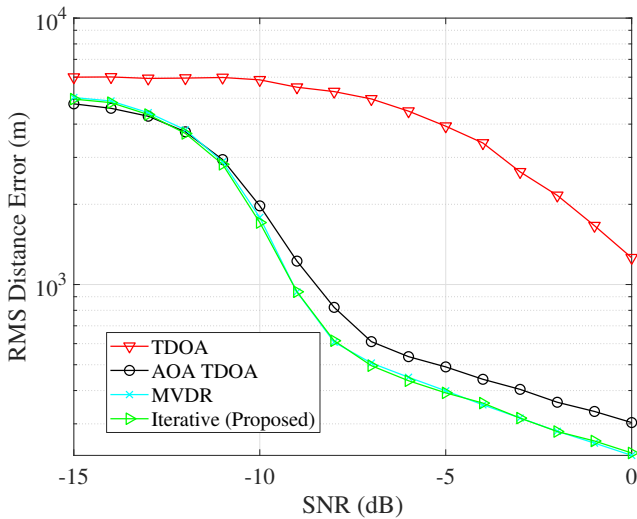


Fig. 11. Highly directive emitter experiment; RMS Distance Error vs SNR, $N = 32$, $M = 4$, $L = 4$, $M_{tx} = 16$.

Significant variations in RSS due to emitter beam pattern are experienced at each receiver. Receivers are placed at locations $[-2500, -2500]$, $[-2500, 2500]$, $[2500, -2500]$, $[2500, 2500]$ m, with transmitter placed at $[500, 500] \pm 250$ m in each coordinate. Transmit orientation is given as $0 \pm 15^\circ$. The setup is illustrated in Fig. 13.

Fig. 14 demonstrates a significant improvement in localization performance under RSS and beam pattern consideration over other techniques. As the leftmost receivers are effectively receiving no information from the emitter, their contributions not only fail to facilitate the estimation, but also hinder it by attempting to correlate noise with le-

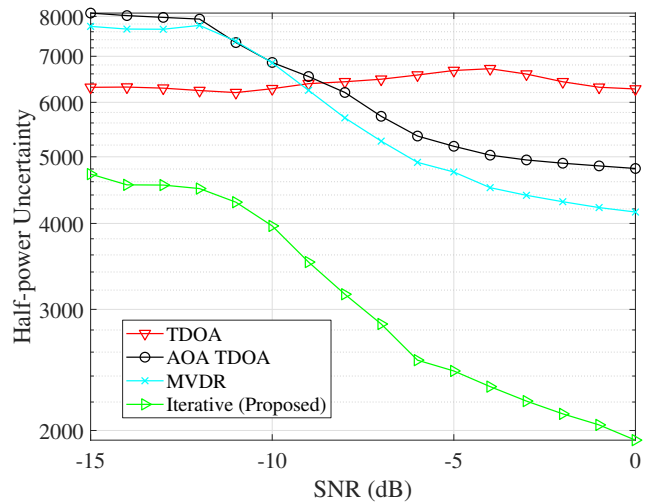


Fig. 12. Highly directive emitter experiment; RMS half-power uncertainty vs SNR, $N = 32$, $M = 4$, $L = 4$, $M_{tx} = 16$.

gitimate measurements. Consideration of the beam pattern effectively weights such receivers' contributions to nil. The non-RSS techniques present a false secondary emitter which is eliminated by the proposed iterative technique. This is of particular value as the second emitter location is qualitatively similar to that of the true emitter which greatly increases uncertainty for critical applications.

RMS distance error (Fig. 15) is dramatically improved by the proposed technique, with non-RSS techniques failing to improve their estimate proportionate to the SNR increase. This is supported by Fig. 16 which similarly shows reduced uncertainty in comparison as expected. The uncertainty decrease for other techniques is disproportionate to their accuracy decrease, suggesting their heatmaps show smaller viable regions but at incorrect locations.

IV. Conclusion

Our method has presented an effective approach for the localization of highly directive emitters by extending the direct position determination model to incorporate the effect of emitter beam pattern. This was achieved by using a modified approach to iteratively estimate beam pattern and position. This approach dramatically improved localization accuracy in two primary scenarios: 1) For a typical directive communication system, and 2) For a highly directive radar system. The presented approach utilizes adaptive beamforming techniques such as MVDR to reduce the impact that spurious noise has on RSS. The iterated approach reduces computational complexity compared to the alternative exhaustive search over position, beam pattern, and orientation.

Notably, the algorithm typically converged within 2 iterations. This process can be further optimized, particularly in determining the initial position estimation at very low signal-to-noise ratios. The process is sensitive to having a poor initial estimate, from which it may not

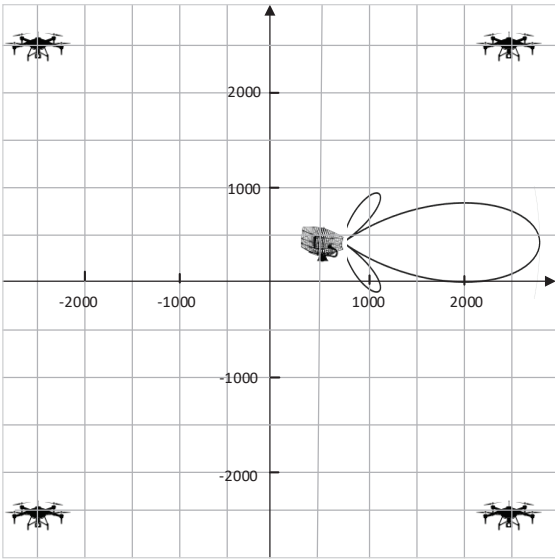


Fig. 13. Directive communication system representative experimental setup.

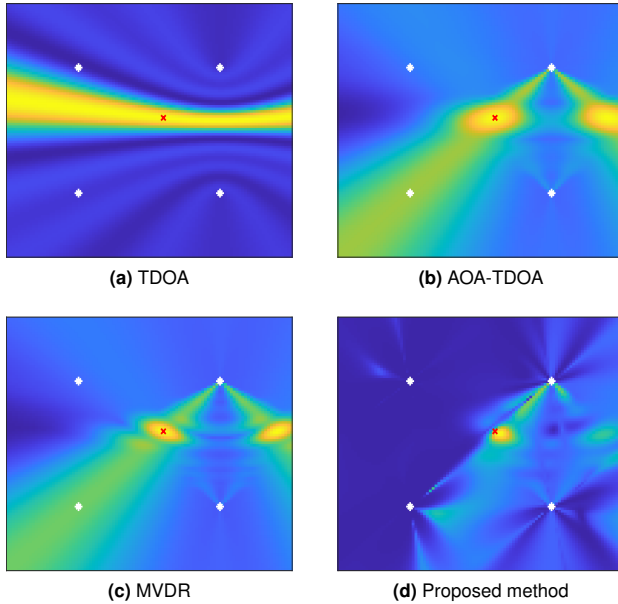


Fig. 14. Directive communication system; Heatmaps of different localization methods with SNR = 30 dB, $N = 32$, $M = 4$, $L = 4$, $M_{tx} = 4$ ULA transmit beampattern. Grids measure 10 km x 10 km. Superimposed white symbols represent receiver positions, and the red cross represents emitter position. (a) TDOA (b) AOA-TDOA (c) MVDR (d) Proposed iterative method.

be able to recover to converge regardless of the number of iterations. Additionally, selecting the beampattern-orientation pair based on the heuristic that the maximum likelihood should correspond to the most angle-robust choice, rather than just the highest likelihood orientation for a specific beampattern, would offer an improvement.

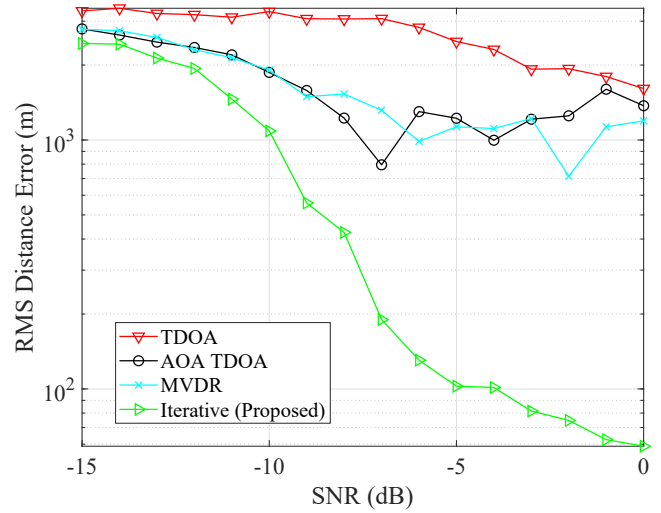


Fig. 15. Directive communication system experiment; RMS distance error vs SNR, $N = 32$, $M = 4$, $L = 4$, $M_{tx} = 16$.

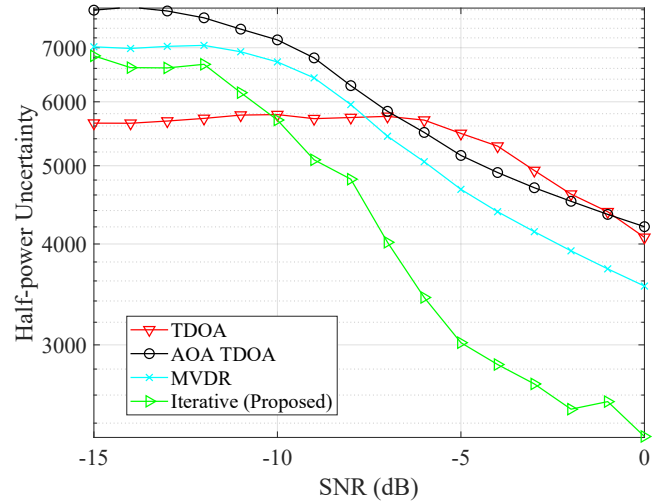


Fig. 16. Directive communication system experiment; RMS half-power uncertainty vs SNR, $N = 32$, $M = 4$, $L = 4$, $M_{tx} = 16$.

REFERENCES

- [1] K. Ho and Y. Chan
Solution and performance analysis of geolocation by TDOA
IEEE Transactions on Aerospace and Electronic Systems, vol. 29, no. 4, pp. 1311–1322, Oct. 1993, conference Name: IEEE Transactions on Aerospace and Electronic Systems.
- [2] A. Weiss
Direct position determination of narrowband radio frequency transmitters
IEEE Signal Processing Letters, vol. 11, no. 5, pp. 513–516, May 2004, conference Name: IEEE Signal Processing Letters.
- [3] C. Liu, J. Yang, and F. Wang
Joint TDOA and AOA location algorithm
Journal of Systems Engineering and Electronics, vol. 24, no. 2, pp. 183–188, Apr. 2013, conference Name: Journal of Systems Engineering and Electronics.
- [4] D. Musicki and W. Koch
Geolocation using TDOA and FDOA measurements
In *2008 11th International Conference on Information Fusion*, Jun. 2008, pp. 1–8.
- [5] Y. Song, C. Hao, M. Li, X. Wang, J. Li, and Q. Wan

A Fast Algorithm of Direct Position Determination Using TDOA and FDOA

Journal of Physics: Conference Series, vol. 1169, p. 012014, Feb. 2019, publisher: IOP Publishing.

- [6] A. Amar and A. J. Weiss
Localization of Narrowband Radio Emitters Based on Doppler Frequency Shifts
IEEE Transactions on Signal Processing, vol. 56, no. 11, pp. 5500–5508, Nov. 2008, conference Name: IEEE Transactions on Signal Processing.
- [7] H. Katabalian, M. Biguesh, and A. Sheikhi
A Closed-Form Solution for Localization Based on RSS
IEEE Transactions on Aerospace and Electronic Systems, vol. 56, no. 2, pp. 912–923, Apr. 2020, conference Name: IEEE Transactions on Aerospace and Electronic Systems.
- [8] M. Y. You, A. N. Lu, Y. X. Ye, and K. Huang
Direct Position Determination Using Compressive Sensing Measurements without Reconstruction
IEEE Transactions on Aerospace and Electronic Systems, pp. 1–8, 2022, conference Name: IEEE Transactions on Aerospace and Electronic Systems.
- [9] N. Salman, M. Ghogho, and A. H. Kemp
On the Joint Estimation of the RSS-Based Location and Path-loss Exponent
IEEE Wireless Communications Letters, vol. 1, no. 1, pp. 34–37, Feb. 2012, conference Name: IEEE Wireless Communications Letters.
- [10] T. S. Rappaport
Wireless communications: principles and practice. Cambridge University Press, 2024.
- [11] M. I. Skolnik
Introduction to radar systems. McGraw-hill New York, 1980, vol. 3.
- [12] M. J. Sibley
Modern telecommunications: Basic principles and practices. CRC Press, 2018.
- [13] F. Williams, D. Jayalath, A. J. Tom, T. Martin, and C. Fookes
Enhancing Emitter Localization Accuracy Through Integration of Received Signal Strength in Direct Position Determination In *2023 IEEE Statistical Signal Processing Workshop (SSP)*. IEEE, 2023, pp. 458–462.
- [14] G. Mao, B. D. O. Anderson, and B. Fidan
Path loss exponent estimation for wireless sensor network localization
Computer Networks, vol. 51, no. 10, pp. 2467–2483, Jul. 2007.
- [15] L. Tzafri and A. J. Weiss
High-Resolution Direct Position Determination Using MVDR
IEEE Transactions on Wireless Communications, vol. 15, no. 9, pp. 6449–6461, Sep. 2016, conference Name: IEEE Transactions on Wireless Communications.



Fraser Williams (Student Member, IEEE) received the B.Eng in electrical engineering and B.Sc in physics from the Queensland University of Technology, Brisbane, Queensland, Australia, in 2021, and is pursuing the Ph.D. in electrical engineering at the same university.

He is currently employed as a Research Engineer at Revolution Aerospace in Brisbane, Queensland, Australia. His research interests include statistical signal processing, array processing, and radio frequency signal processing.



Akila Pemasiri received her B.Sc. degree in Computer Science and Engineering from the University of Moratuwa, Sri Lanka, and her Ph.D. from the Queensland University of Technology (QUT), Australia, in 2021. She is currently a Postdoctoral Research Fellow in the Signal Processing, Artificial Intelligence, and Vision Technologies group at QUT. Her research interests include applying machine learning principles to solve complex problems across various domains, including communications, defense, medical and healthcare, sports, and infrastructure.



Dhammika Jayalath (Senior Member, IEEE) received the B.Sc. degree in electronics and telecommunications engineering from the University of Moratuwa, Sri Lanka, the M.Eng. degree in telecommunications from the Asian Institute of Technology, Thailand, and the Ph.D. degree in wireless communications from Monash University, Australia, in 2002. He was a fellow with the Australian National University and a Senior Researcher with the National ICT Australia. He has been an Academician with the Science and Engineering Faculty, Queensland University of Technology, since 2007. His research interests include the general areas of communications and signal processing. He has published significantly in these areas. His current research interests include applying machine learning principles in communication systems, physical layer security, and signal design for robust communications.



Terrence Martin is a co-founder of Revolution Aerospace. He is a former RAAF & Army military aerospace engineering officer with a PhD in Applied Signal Processing & Machine Learning. He has accumulated significant experience across a 35-year career-span, with time on fast jets & rotary wing manned platforms, alongside an extensive array of work for RAAF, Navy & Army on a variety of UAV platforms. Terry has a deep interest in UAV related technologies, and in 2018 he was nominated by Engineers Australia as one of Australia's 30 most Innovative Engineers.



Clinton Fookes (Senior Member, IEEE) received the B.Eng. in Aerospace and Avionics, the MBA degree, and the Ph.D. degree in computer vision. He is currently the Associate Dean Research and a Professor of Vision and Signal Processing with the Faculty of Engineering at the Queensland University of Technology, Brisbane, Australia. His research interests include computer vision, machine learning, signal processing, and artificial intelligence. He serves on the editorial boards for IEEE TRANSACTIONS ON IMAGE PROCESSING and Pattern Recognition. He has previously served on the Editorial Board for IEEE TRANSACTIONS ON INFORMATION FORENSICS AND SECURITY. He is a Fellow of the International Association of Pattern Recognition and a Fellow of the Australian Academy of Technological Sciences and Engineering. He is a Senior Member of the IEEE and a multi-award winning researcher including an Australian Institute of Policy and Science Young Tall Poppy, an Australian Museum Eureka Prize winner, Engineers Australia Engineering Excellence Award, Australian Defence Scientist of the Year, and a Senior Fulbright Scholar.